

# New family of quasi-Hermitian Hamiltonians and its application in coupled predator-prey circles

Tengzhou Zhang<sup>1</sup> and Zi Cai<sup>1,2,\*</sup>

<sup>1</sup>*Wilczek Quantum Center and Key Laboratory of Artificial Structures and Quantum Control, School of Physics and Astronomy, Shanghai Jiao Tong University, Shanghai 200240, China*

<sup>2</sup>*Shanghai Research Center for Quantum Sciences, Shanghai 201315, China*

Herein, we propose a family of non-Hermitian Hamiltonians with real spectra other than the space-time reflection (PT) symmetric class, and discuss its application in the predator-prey ecological processes described by a generalized Lotka-Volterra equation. In the phase space, such a nonlinear equation could support both chaotic and localized dynamics separated by a dynamical critical point, which can be understood as a consequence of the interplay between the periodicity and non-Hermiticity of its effective Hamiltonian in the linearized equation of motion. Further, the dynamics at the critical point (*e.g.* the algebraic divergence,) can be understood as an exceptional point in the context of non-Hermitian physics. Applications to genuine quantum systems have also been discussed.

*Introduction* –As a standard axiom of quantum mechanics, the Hermiticity of a Hamiltonian guarantees the real-valuedness of an energy spectrum as well as the probability conservation in an isolated quantum system. However, the Hermiticity requirement can be replaced by a physically transparent condition of space-time reflection (PT) symmetry, while the essential features of quantum mechanics are preserved[1, 2]. More general mathematical conditions for a non-Hermitian Hamiltonian with real energy spectrum (dubbed quasi-Hermitian) have also been discussed[3, 4]. Physically, non-Hermitian Hamiltonians[5], as a phenomenological description of process with energy or particle flowing out of the Hilbert space of interest, are responsible for diverse intriguing phenomena in the contexts of classical and quantum waves[6–11], topological physics[12–18], and active matters[19]. Searching for physically transparent examples of non-Hermitian Hamiltonian with real energy spectra is not only of fundamental interest for exploring non-Hermitian physics in a broader context, but also of practical significance due to its potential application in quantum sensing[20, 21] and energy transfer[22–24].

To this end, we propose a new class of non-Hermitian systems, whose Hamiltonian  $H$  can be expressed in terms of a product of two matrices as

$$H = VD, \quad (1)$$

where both  $D$  and  $V$  represent Hermitian matrices and at least one of them is positive definite. In general,  $D$  and  $V$  do not commute with each other, thus  $H$  is non-Hermitian. However, the real-valuedness of the eigenvalues of  $H$  can be easily proved as follows: assuming that  $\mathbf{x}$  is the eigenstate of  $H$  with eigenvalue  $\lambda$ :

$$H\mathbf{x} = \lambda\mathbf{x}. \quad (2)$$

According to Cholesky decomposition, a positive definite Hermitian matrix can always be factorized into a product of a lower triangular matrix and its conjugate transpose:  $D = LL^\dagger$ [25]; hence, we have  $H = VLL^\dagger$ . By operating

$L^\dagger$  on both sides of Eq.(2) one can obtain:

$$\tilde{H}\mathbf{y} = \lambda\mathbf{y} \quad (3)$$

where  $\mathbf{y} = L^\dagger\mathbf{x}$  and  $\tilde{H} = L^\dagger VL$  is a Hermitian matrix ( $\tilde{H} = \tilde{H}^\dagger$ ). Eq.(2) and (3) indicate that for a given non-Hermitian Hamiltonian  $H$  satisfying Eq.(1), one can always find a Hermitian Hamiltonian  $\tilde{H}$ , which shares the same set of eigenvalues with  $H$ . Therefore, the eigenvalues of  $H$  also have to be real. Despite the conciseness of this mathematical proof, finding a physical system whose Hamiltonian satisfies Eq.(1) is non-trivial, because the physical meaning of multiplication of two operators is elusive in quantum mechanics.

In this paper, we propose a generalized Lotka-Volterra equation (GLVE) in a one-dimensional (1D) lattice, which could exhibit chaotic or stable dynamics in different parameter regimes. The Lotka-Volterra (LV) equation describing the predator-prey ecological processes is a paradigmatic model in population dynamics[26–28]. Recently, the GLVE has been generalized to spatially periodic systems to study the topological phases and edge modes beyond the scope of natural science[29–31]. The dynamics of a slight deviation from the stationary point of the GLVE are governed by a linearized equation resembling the single-particle Schrodinger equation in a lattice system. Therefore, the topological band theory can straightforwardly be applied to such a classical system[29, 30]. Here, we show that if the linear expansion is performed around a temporal periodic solution instead of the stationary point of the GLVE, the equation of motion (EOM) of the deviation can also be described by the Schrodinger equation, but with a time-dependent Hamiltonian which is generally non-Hermitian but satisfies Eq.(1). The dynamical critical point in the original nonlinear model can be understood as an exceptional point for the effective non-Hermitian Floquet Hamiltonian.

*Model and method* – We focus on the GLVE defined in

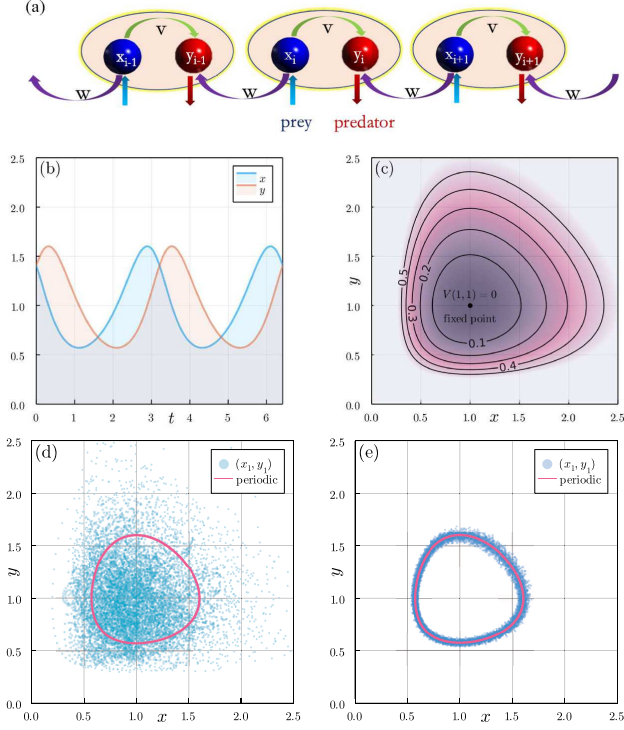


FIG. 1: (Color online)(a) Predator-prey model defined in a 1D “diatomic” chain described by the GLVE.(4). (b) Periodic solution  $[\bar{x}(t), \bar{y}(t)]^T$  of the homogeneous GLVE.(5) with the conserved quantity  $V = 0.131$ . (c) Trajectories of  $[\bar{x}(t), \bar{y}(t)]^T$  in the phase space with different conserved quantities. (d) and (e) Trajectories in the phase space of the first unit cell ( $i = 1$ ) predicted via the GLVE.(4) with (d)  $r = 0.3$  and (e)  $r = 0.7$ ,  $\Delta = 0.05$  and  $L = 1024$ . The initial state of (d) and (e) is spatially inhomogeneous:  $\delta_i(t = 0) = \Delta_i$  with  $\Delta_i$  being randomly sampled from  $[-\Delta, \Delta]$ . The red curves indicate the trajectory starting from the spatially homogeneous initial state  $\delta_i(t = 0) = 0$ .

a 1D “diatomic” chain (see Fig.1 a), which reads:

$$\begin{aligned}\dot{x}_i &= x_i[2 - vy_{i-1} - wy_i] \\ \dot{y}_i &= y_i[-2 + vx_i + wx_{i+1}]\end{aligned}\quad (4)$$

where  $i = 1 \dots L$ , and  $L$  is the number of the unit cell, each of which contains a prey ( $x_i$ ) and predator ( $y_i$ ).  $v = 1 + r$  and  $w = 1 - r$ .  $0 < r < 1$  is the only tunable parameter in Eq.(4) characterizing the difference between the inter and intra unit cell coupling strengths. The linear terms in the right side of Eq.(4) suggest an exponential growth/decay for the prey/predator populations if there is no interspecies interaction, while the nonlinear terms indicate the interaction between one specie and its neighbors, which suppress the exponential growth/decay.

Starting with a simple situation where the populations of prey and predator are site-independent  $x_i(t) = x(t)$ ,  $y_i(t) = y(t)$ , Eq.(4) is reduced to a two-species LV equa-

tion:

$$\begin{aligned}\dot{x} &= 2x - 2xy \\ \dot{y} &= -2y + 2xy\end{aligned}\quad (5)$$

which was used to explain the oscillation behavior of natural populations (*e.g.* the snowshoe hare and lynx) in ecological systems with predator-prey interactions, competition and disease. Mathematically, this model is integrable with a constant of motion  $V = x + y - \ln xy - 2$ [28]. Consequently, it supports either a steady solution  $[1, 1]^T$  (with  $V = 0$ ) or a periodic oscillation  $[\bar{x}(t), \bar{y}(t)]^T$  ( $V > 0$ ) (see Fig.1 b), corresponding to a fixed point or a closed orbit around the fixed point in the phase space respectively (see Fig.1 c).

In general, one needs to take the spatial fluctuation into account. Considering a solution  $\mathbf{v}(t) = [x_1, y_1, \dots, x_L, y_L]^T$  of Eq.(4), one can expand it around the spatially homogeneous solutions as

$$\mathbf{v}(t) = [1 + \boldsymbol{\delta}(t)]\bar{\mathbf{v}}(t) \quad (6)$$

with  $\boldsymbol{\delta}(t) = [\delta_1^x(t), \delta_1^y(t), \dots]^T$  ( $\delta_i^x(t) = \frac{x_i(t) - \bar{x}(t)}{\bar{x}(t)}$  and  $\delta_i^y(t)$  is likewise). A linearized equation can be derived in terms of the dimensionless vector  $\boldsymbol{\delta}(t)$ . For a homogeneous stationary solution  $\bar{\mathbf{v}}_s(t) = [1, 1, \dots, 1, 1]^T$ , it is shown that the linearized EOM of  $\boldsymbol{\delta}(t)$  takes the identical form of the single-particle Schrodinger equation in a 1D lattice:

$$i \frac{d\boldsymbol{\delta}(t)}{dt} = H\boldsymbol{\delta}(t) \quad (7)$$

where  $H = H_0$  is a time-independent  $2L \times 2L$  antisymmetric Hermitian matrix:

$$H_0 = i \begin{bmatrix} 0 & -v & & -w \\ v & 0 & w & \\ & -w & 0 & -v \\ & & v & 0 & \ddots \\ w & & & \ddots & \ddots \end{bmatrix} \quad (8)$$

Unlike previous studies[29, 30], here we expand the nonlinear Eq.(4) around the periodic solution  $\bar{\mathbf{v}}_p(t) = [\bar{x}(t), \bar{y}(t), \dots, \bar{x}(t), \bar{y}(t)]^T$ , where  $\bar{x}(t), \bar{y}(t)$  are the solution of Eq.(5) with a period  $T = \pi$ . The linearized EOM takes the same form of Eq.(7), but with a time-dependent “Hamiltonian”

$$H(t) = H_0 D(t), \quad (9)$$

where  $H_0$  has the same definition as Eq.(8), and  $D(t)$  is a diagonal matrix with dimension  $2L$ :

$$D(t) = \begin{bmatrix} \bar{x}(t) & & & \\ & \bar{y}(t) & & \\ & & \ddots & \\ & & & \bar{x}(t) \\ & & & & \bar{y}(t) \end{bmatrix} \quad (10)$$

Generally,  $H_0$  and  $D(t)$  are Hermitian, and  $D(t)$  is positive definite because  $\bar{x}(t)$  and  $\bar{y}(t)$  are positive. Therefore, although  $H(t)$  is non-Hermitian, it satisfies the condition presented in Eq.(1), thus its instantaneous eigenvalues are real.

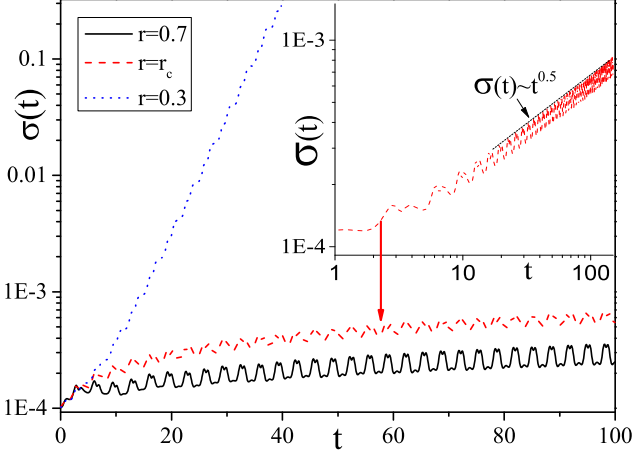


FIG. 2: (Color online) Dynamics of the average deviation  $\bar{\sigma}(t)$  with different  $r$  values in a semi-log plot ( $r_c = 0.64579$  is the critical point). The inset presents the dynamics of  $\bar{\sigma}(t)$  at the critical point in the log-log plot. The initial state is chosen as  $x_i(t=0) = y_i(t=0) = 1.6(1 + \Delta_i)$ , where  $\Delta_i$  is randomly sampled from  $[-\Delta, \Delta]$  and  $\Delta = 2 \times 10^{-4}$ .

*Chaotic versus localized dynamics in the phase space* – Before discussing the linearized EOM, we first focus on the dynamics of the nonlinear Eq.(4), which can be solved using the standard Runge-Kutta method. A key question is whether the spatially homogeneous periodic solution  $[\bar{x}(t), \bar{y}(t)]^T$  is stable against spatial fluctuations. To address this issue, we impose a small site-dependent perturbation on the initial state as  $\delta_i(t=0) = \Delta_i$ , where  $\Delta_i$  is randomly sampled from a uniform random distribution with  $\Delta_i \in [-\Delta, \Delta]$  and  $\Delta \ll 1$  (for a spatially homogeneous solution  $\delta_i(t=0) = 0$ ). We first study the dynamics in one unit cell (say,  $i = 1$ ) by plotting the trajectories of  $x_1(t)$  and  $y_1(t)$  in the phase space. As shown in Fig.1 (d), for a small  $r$  (e.g.  $r = 0.3$ ), the trajectory of  $[x_1(t), y_1(t)]^T$  rapidly deviates from the spatially homogeneous solution  $[\bar{x}(t), \bar{y}(t)]^T$  after a short time, while randomly walking in the phase space on long timescales, indicating that the solution  $[\bar{x}(t), \bar{y}(t)]^T$  is unstable against spatial fluctuation for small  $r$ . Conversely, at a relatively large  $r$  (e.g.  $r = 0.7$ ), the trajectory of  $[x_1(t), y_1(t)]^T$  is bounded within a finite regime around  $[\bar{x}(t), \bar{y}(t)]^T$  (see Fig.1 e), which resembles the Kolmogorov-Arnold-Moser theorem[32].

The qualitatively different dynamical behavior between the cases with small and large values of  $r$  reveal a dynamical phase transition, which can be characterized by the average deviation:  $\bar{\delta}(t) =$

$\sqrt{\frac{1}{L} \sum_i [\delta_i^x(t)]^2 + [\delta_i^y(t)]^2}$ . As shown in Fig.2,  $\bar{\delta}(t)$  increases exponentially (accompanied by an oscillation) at small  $r$  (a signature of chaos), while it keeps oscillating around a finite value at a large  $r$ . The exponent of the exponential divergence approaches zero at critical  $r = r_c$ , whose value depends on the amplitude of the periodic oscillation of the spatially homogeneous solutions. At the dynamical critical point,  $\bar{\delta}(t)$  grows algebraically as  $\bar{\delta}(t) \sim t^{\frac{1}{2}}$ . In the following, we will explain these observed dynamical behaviors as well as the critical dynamics based on the properties of the non-Hermitian Hamiltonian in Eq.(9).

*Floquet dynamics with a non-Hermitian Hamiltonian* – Now we focus on the linearized EOM.(7) where the time-dependent Hamiltonian (9) is non-Hermitian but periodic in time  $H(t) = H(t+T)$ . However, unlike the intensively studied cases with periodically driven Hamiltonian, the periodic oscillation in Hamiltonian (9) is not due to external driving, but originates from the spontaneous oscillation in the time-independent GLVE.(4), and is self-sustained. Thanks to the spatially translational invariance, one can perform the Fourier transformation, after which the EOM.(7) turns into a collection of independent  $k$  modes, each of which is a two-level system governed by the EOM:

$$i \frac{d\delta_k}{dt} = H_k(t) \delta_k \quad (11)$$

where  $\delta_k = [\delta_k^x, \delta_k^y]^T$  with  $\delta_k^x = \frac{1}{\sqrt{L}} \sum_j e^{-ikj} \delta_j^x$  and  $\delta_k^y$  is likewise.  $H_k$  is a  $2 \times 2$  matrix defined as:

$$H_k(t) = H_k^0 D(t) \quad (12)$$

with

$$H_k^0 = \begin{bmatrix} 0 & -i(v + we^{-ik}) \\ i(v + we^{ik}) & 0 \end{bmatrix}, D(t) = \begin{bmatrix} \bar{x}(t) & \\ & \bar{y}(t) \end{bmatrix} \quad (13)$$

Again,  $H_k$  is non-Hermitian if  $\bar{x}(t) \neq \bar{y}(t)$ , but its instantaneous eigenvalues are real because it satisfies the condition (1). Both  $\bar{x}(t)$  and  $\bar{y}(t)$  are periodic in time with a period  $T$ , enabling us to employ the Floquet description of the stroboscopic dynamics of Eq.(11) and derive a time-independent Floquet Hamiltonian  $H_k^F$  satisfying:

$$\mathcal{F}_k = e^{-iH_k^F T} = \mathcal{T} e^{-i \int_0^T dt H_k(t)} \quad (14)$$

where  $\mathcal{T}$  is the time-ordering operator and  $\mathcal{F}_k$  is the evolution operator for the  $k$ -mode within one period.

Because the explicit formalism of the periodic solution  $[\bar{x}(t), \bar{y}(t)]^T$  is complex, to derive an analytic formalism of  $H_k^F$ , we replace the diagonal matrix in Eq.(34) by a simplified formalism as[33]:

$$D(t) = \begin{cases} \mathbb{I} + \xi \hat{\sigma}^z, & nT < t < (n + \frac{1}{2})T \\ \mathbb{I} - \xi \hat{\sigma}^z, & (n + \frac{1}{2})T < t < (n + 1)T \end{cases} \quad (15)$$

where  $n$  is an integer,  $\mathbb{I}$  represents a  $2 \times 2$  unit matrix and  $\hat{\sigma}^z$  denotes the  $z$ -component Pauli matrix. Furthermore,

$\xi \in [0, 1]$  characterizes the amplitude of the periodic oscillation, which is determined by the initial conditions in the original LV equation. In the following, we demonstrate that despite the simplicity of such a step-function approximation, it can capture the essence of the non-Hermitian Floquet physics, and explain the numerical results observed in the nonlinear Eq.(4). By introducing  $H_k^\pm = H_k^0(\mathbb{I} \pm \xi \sigma_z)$ , the evolution operator becomes

$$\mathcal{F}_k = e^{-i\frac{T}{2}H_k^+} e^{-i\frac{T}{2}H_k^-} = \begin{bmatrix} \frac{\cos \phi_k + \xi}{1 + \xi} & -\frac{ie^{i\varphi_k} \sin \phi_k}{\sqrt{1 - \xi^2}} \\ -\frac{ie^{-i\varphi_k} \sin \phi_k}{\sqrt{1 - \xi^2}} & \frac{\cos \phi_k - \xi}{1 - \xi} \end{bmatrix} \quad (16)$$

where  $\phi_k = \frac{\Delta_k T}{2} \sqrt{1 - \xi^2}$  and  $\Delta_k$  is the energy gap of  $H_k^0$  ( $\Delta_k = 2\sqrt{(2 + 2\cos k) + 2(1 - \cos k)r^2}$ ).  $\varphi_k = \arg[-i(v + we^{-ik})]$ . By diagonalizing the matrix presented in Eq.(16), one can obtain the eigenvalues of  $\mathcal{F}_k$ :

$$\lambda_k = \frac{\cos \phi_k - \xi^2 \pm 2i \sin \frac{\phi_k}{2} \sqrt{\cos^2 \frac{\phi_k}{2} - \xi^2}}{1 - \xi^2} \quad (17)$$

Notably, the properties of  $\lambda_k$  considerably depend on the sign of  $\cos^2 \frac{\phi_k}{2} - \xi^2$ , resulting in qualitatively different physical consequences. If  $\cos^2 \frac{\phi_k}{2} > \xi^2$  for all the k-modes, it is easy to check that  $|\lambda_k| = 1$ , therefore we can introduce a real number  $\theta_k \in [0, 2\pi]$  such that  $\lambda_k = e^{\pm i\theta_k}$ . Let  $\epsilon_k$  be the quasi-energy of the Floquet Hamiltonian  $H_k^F$ , since  $H_k^F = \frac{i}{T} \ln \mathcal{F}_k$ , one can obtain  $\epsilon_k = \frac{i}{T} \ln \lambda_k = \mp \frac{\theta_k}{T}$ . Therefore, in this case all the eigenvalues of the Floquet Hamiltonian  $H_k^F$  are real and the stroboscopic dynamics are stable. Consequently, there is no divergence for the deviation, and the dynamics is bounded within a finite regime around the homogeneous trajectory  $[\bar{x}(t), \bar{y}(t)]$ , agreeing with our numerical observation for large  $r$ .

The energy gap of  $H_0^k$  satisfies  $\Delta_k \in [4r, 4]$  ( $0 < r < 1$ ), which takes its minimum value  $\Delta_{\min} = 4r$  at  $k = \pi$ . Therefore, for a fixed by small oscillation amplitude  $\xi$ , the  $\pi$ -mode ( $k = \pi$ ) will first become unstable when  $r$  is below the critical value  $r_c$  satisfying  $\cos[\pi r_c \sqrt{1 - \xi^2}] = -\xi$ , which indicates that  $r_c \rightarrow \frac{1}{2}$  in the limit  $\xi \rightarrow 0$ . For  $r > r_c$ ,  $\lambda_k$  defined in Eq.(17) becomes real and  $|\lambda_k| \neq 1$ . As a consequence, the eigenvalue of the Floquet Hamiltonian  $\epsilon_k$  is no longer real, but with a pair of opposite imaginary parts, which is responsible for the exponential divergence of the deviation observed in the case with small  $r$ . Obviously, such an exponential divergence predicted by the linear analysis cannot persist forever, because the nonlinear effect will finally take over and governs the long-time dynamics.

*Critical dynamics: an algebraic divergence*– Right at the critical point  $|\cos \frac{\phi_\pi}{2}| = \xi$ , the Floquet evolution operator for the  $\pi$ -mode presented in Eq.(16) become

$$\mathcal{F}_\pi = 2\xi \begin{bmatrix} 1 & -1 \\ 1 & -1 \end{bmatrix} + \begin{bmatrix} -1 & 0 \\ 0 & -1 \end{bmatrix} \quad (18)$$

Such a  $2 \times 2$  matrix has only one eigenvector with eigenvalue  $\lambda_\pi = -1$ , indicating it is an exceptional point for the non-Hermitian matrix  $\mathcal{F}_k$ . The Floquet evolution operator presented in Eq.(24) suggests that  $\delta_\pi(nT) = \mathcal{F}_\pi^n \delta_\pi(0)$ . One can prove that at the critical point, the  $\pi$ -mode grows linearly in time[33]. To explain the algebraic divergence of the average deviation  $\bar{\sigma}(t) \sim t^{\frac{1}{2}}$  observed at the critical point, the dynamics of k-modes close to  $k = \pi$  must be considered. Right at the critical point, only the  $\pi$ -mode grows linearly, while for other k-modes close to  $\pi$ -mode ( $k = \pi + q$  with  $|q| \ll 1$ ), they will first grow linearly with time up to a saturate time scale  $t_k^*$  ( $\delta_k(t) \sim t$  for  $t < t_k^*$ ), after which their dynamics start to significantly deviate from the linear growth[33]. For a k-mode with  $k = \pi + q$ , its saturated time scale  $t_k^* \sim 1/|q|$  ( $t_k^* \rightarrow \infty$ ). As a consequence, at a given time  $t$ , only those k-modes satisfying  $t_k^* > t$  are still growing linearly, and their number decreases with time as  $\mathcal{N}(t) \sim 1/t$ [33]. Therefore, these modes close to the  $\pi$ -mode dominate the long-time dynamics and the average deviation can be expressed as:

$$\bar{\sigma}(t) = \sqrt{\frac{1}{L} \sum_k \delta_k(t) \delta_{-k}(t)} \sim \sqrt{\mathcal{N}(t) \delta_{\pi+q}(t) \delta_{\pi-q}(t)} \sim t^{\frac{1}{2}} \quad (19)$$

which agrees with the  $t^{\frac{1}{2}}$  divergence observed at the critical point in the original GLVE.

*Discussion* – Finally, we discuss the relationship between our results and the well-studied cases with the PT symmetric, or more generally, pseudo-Hermitian Hamiltonian. In general, the condition in Eq.(1) does not have to be related to the PT symmetry. However, in the proposed model, the original nonlinear Eq.(4) is indeed invariant under the PT transformation:  $x_i \rightarrow y_{L-i}$ ,  $y_i \rightarrow x_{L-i}$  and  $t \rightarrow -t$ . However, once we perform the expansion around the periodic solution and derive the linearized EOM.(7), the effective Hamiltonian  $H$  becomes time-dependent (periodic), and breaks the time-reversal symmetry ( $D(t) \neq \pm D(-t)$ ). Although  $H$  is not PT symmetric, it satisfies the condition presented in Eq.(1), thus its instantaneous energy spectra are real, although its Floquet quasi-energy spectra could be complex. Mathematically, the non-Hermitian Hamiltonian satisfying Eq.(1) can be proved to belong to a subclass of pseudo-Hermitian Hamiltonian[33], while the proposed GLVE provides a realistic example of this type of non-Hermitian Hamiltonian and make it physically feasible.

*Conclusion and outlook* – In summary, we proposed a class of non-Hermitian Hamiltonian with real spectra other than the PT symmetric class. The Floquet dynamics of such a non-Hermitian system was studied in the context of an GLVE, where we found a dynamical phase transition characterized by an EP point. Although its EOM.(7) shared the identical formalism as the Schrodinger equation, the proposed system is classical. Therefore, a question arises whether this type of non-Hermitian Hamiltonian satisfying Eq.(1) can be applied to genuine quantum systems, *e.g.* in a quantum circuit



system simulating the imaginary time evolution[34, 35], where the Hermitian operators  $V$  and  $D$  in Eq.(1) can be understood as the imaginary time propagators with different Hamiltonians. Another possible application of our results is in the quadratic bosonic system, whose Hamiltonian is Hermitian. However, owing to the commutation relation between the bosonic operators, the corresponding Bogoliubov-de Gennes equation resembles a Schrodinger equation but with a non-Hermitian Hamiltonian, which falls into the category defined in Eq.(1)[33]. Such a similarity allows us to explore the intriguing phenomena originated in non-Hermitian physics (*e.g.* the skin effect) in such a Hermitian quantum system[36–38]. Finally, this study revealed that the interplay between temporal periodicity and non-Hermiticity may lead to intriguing dynamical behaviors, shedding light on investigating the periodically-driven non-Hermitian systems[39–44].

*Acknowledgments.*—This work is supported by the National Key Research and Development Program of China (Grant No. 2020YFA0309000), NSFC of China (Grant No.12174251), Natural Science Foundation of Shanghai (Grant No.22ZR142830), Shanghai Municipal Science and Technology Major Project (Grant No.2019SHZDZX01). ZC thank the sponsorship from Yangyang Development Fund.

---

\* Electronic address: zcai@sjtu.edu.cn

- [1] C. M. Bender and S. Boettcher, Phys. Rev. Lett. **80**, 5243 (1998).
- [2] C. M. Bender, Reports on Progress in Physics **70**, 947 (2007).
- [3] A. Mostafazadeh, J. Math. Phys. **43**, 205 (2002).
- [4] A. Mostafazadeh, J. Math. Phys. **43**, 2814 (2002).
- [5] Y. Ashida, Z. Gong, and M. Ueda, Advances in Physics **69**, 249 (2020).
- [6] A. Ruschhaupt, F. Delgado, and J. G. Muga, Journal of Physics A: Mathematical and General **38**, L171 (2005).
- [7] C. E. Ruter, K. G. Makris, R. El-Ganainy, D. N. Christodoulides, M. Segev, and D. Kip, Nat. Phys. **6**, 192 (2010).
- [8] B. Peng, S.K.Ozdemir, F. Lei, F. Monifi, M. Gianfreda, G. L. Long, S. H. Fan, F. Nori, C. M. Bender, and L. Yang, Nat. Phys. **10**, 394 (2014).
- [9] L. Feng, Z. J. Wong, R. M. Ma, Y. Wang, and X. Zhang, Science **346**, 972 (2014).
- [10] K. Bertoldi, V. Vitelli, J. Christensen, and M. van Hecke, Nat. Rev. Mater. **2**, 17066 (2017).
- [11] L. Xiao, T. Deng, K. Wang, G. Zhu, Z. Wang, W. Yi, and P. Xue, Phys. Rev. **16**, 761 (2020).
- [12] T. E. Lee, Phys. Rev. Lett. **116**, 133903 (2016).
- [13] S. Yao and Z. Wang, Phys. Rev. Lett. **121**, 086803 (2018).
- [14] S. Yao, F. Song, and Z. Wang, Phys. Rev. Lett. **121**, 136802 (2018).
- [15] Z. Gong, Y. Ashida, K. Kawabata, K. Takasan, S. Higashikawa, and M. Ueda, Phys. Rev. X **8**, 031079 (2018).
- [16] C.-H. Liu, H. Jiang, and S. Chen, Phys. Rev. B **99**, 125103 (2019).
- [17] E. J. Bergholtz, J. C. Budich, and F. K. Kunst, Rev. Mod. Phys. **93**, 015005 (2021).
- [18] X.-R. Wang, C.-X. Guo, and S.-P. Kou, Phys. Rev. B **101**, 121116 (2020).
- [19] M. Fruchart, R. Hanai, P. B. Littlewood, and V. Vitelli, Nature **592**, 363 (2021).
- [20] W. Chen, S.K.Ozdemir, G. Zhao, J. Wiersig, and L. Yang, Nature **748**, 192 (2017).
- [21] H. Hodaei, A. U. Hassan, S. Wittek, H. Garcia-Gracia, R. El-Ganainy, D. N. Christodoulides, and M. Khajavikhan, Nature **548**, 187 (2017).
- [22] S. Assaworrorarit, X.Yu, and S. Fan, Nature **546**, 387 (2017).
- [23] H. Xu, D. Mason, L. Jiang, and J. G. E. Harris, Nature **537**, 80 (2016).
- [24] J. C. Budich and E. J. Bergholtz, Phys. Rev. Lett. **125**, 180403 (2020).
- [25] R. Horn and C. R. Johnson, *Matrix Analysis* (Cambridge University Press, Cambridge, 1985).
- [26] A.J.Lotka, J. Phys. Chem **14**, 271 (1910).
- [27] J. Volterra, J. Cons. Perm. Int. Explor. Mer **3**, 1 (1928).
- [28] N. S. Goel, S. C. Maitra, and E. W. Montroll, Rev. Mod. Phys. **43**, 231 (1971).
- [29] J. Knebel, P. M. Geiger, and E. Frey, Phys. Rev. Lett. **125**, 258301 (2020).
- [30] T. Yoshida, T. Mizoguchi, and Y. Hatsugai, Phys. Rev. E **104**, 025003 (2021).
- [31] E. Tang, J. Agudo-Canalejo, and R. Golestanian, Phys. Rev. X **11**, 031015 (2021).
- [32] V.I.Arnold, *Mathematical Methods of Classical Mechanics*, 2nd ed., Appendix 8 (Springer, 1997).
- [33] See the supplementary material for details of the step function approximation and the corresponding phase diagram, an analytic study of the critical dynamics, a proof of pseudo-Hermiticity as well as an application of our results in the quadratic bosonic systems.
- [34] S. McArdle, T. Jones, S. Endo, Y. Li, S. C. Benjamin, and X. Yuan, NPJ Quantum information **5**, 75 (2019).
- [35] S.-H. Lin, R. Dilip, A. G. Green, A. Smith, and F. Pollmann, PRX Quantum **2**, 010342 (2021).
- [36] A. McDonald, T. Pereg-Barnea, and A. A. Clerk, Phys. Rev. X **8**, 041031 (2018).
- [37] V. P. Flynn, E. Cobanera, and L. Viola, New Journal of Physics **22**, 083004 (2020).
- [38] K. Yokomizo and S. Murakami, Phys. Rev. B **103**, 165123 (2021).
- [39] J. Li, A. K. Harter, J. Liu, Y. N. J. Leonardo de Melo and, and L. Luo, Nature Communication **10**, 855 (2019).
- [40] S. Longhi, Journal of Physics A: Mathematical and Theoretical **50**, 505201 (2017).
- [41] T. T. Koutserimpas and R. Fleury, Phys. Rev. Lett. **120**, 087401 (2018).
- [42] B. Höckendorf, A. Alvermann, and H. Fehske, Phys. Rev. Lett. **123**, 190403 (2019).
- [43] H. Wu and J.-H. An, Phys. Rev. B **102**, 041119 (2020).
- [44] X. Zhang and J. Gong, Phys. Rev. B **101**, 045415 (2020).

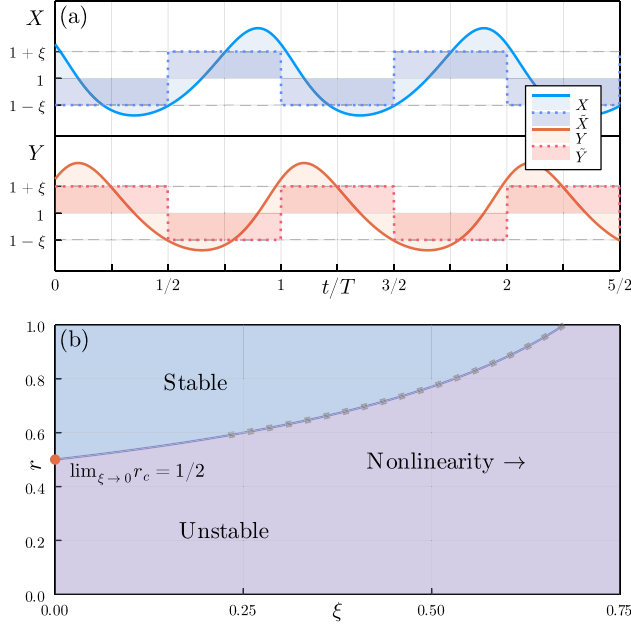


FIG. 3: (Color online) (a) Sketch of the step-function approximation where the periodic solution  $[\bar{x}(t), \bar{y}(t)]^T$  are replaced by the step functions  $[\tilde{x}(t), \tilde{y}(t)]^T$  (b) the phase diagram in the simplified model

## Supplementary material for “New family of quasi-Hermitian Hamiltonian and its application in coupled predator-prey circles”

We first provide the details of the step-function approximation as well as the corresponding phase diagram. The critical dynamics has been studied analytically. We also prove the pseudo-Hermiticity of the proposed Hamiltonian, and discussed its application in the quadratic bosonic systems.

### STEP-FUNCTION APPROXIMATION AND THE CORRESPONDING PHASE DIAGRAM

In the main text, to derive the analytic formalism of the Floquet evolution operator  $\mathcal{F}_k$ , we adopted the step-function approximation where we replaced the original diagonal matrix

$$D(t) = \begin{bmatrix} \bar{x}(t) \\ \bar{y}(t) \end{bmatrix} \quad (20)$$

by a step function:

$$D(t) = \begin{cases} \mathbb{I} + \xi \hat{\sigma}^z, & nT < t < (n + \frac{1}{2})T \\ \mathbb{I} - \xi \hat{\sigma}^z, & (n + \frac{1}{2})T < t < (n + 1)T \end{cases} \quad (21)$$

as shown in Fig.3 (a). Taking the advantage of this approximation, we don't need to perform the time-order

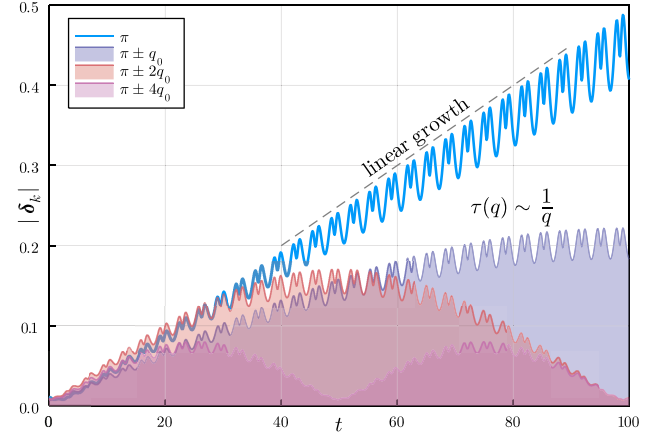


FIG. 4: (Color online) The dynamics of  $|\sigma_k|$  for different k-modes that are right at or close to  $k = \pi$ .  $q_0 = \frac{\pi}{64}$

product to calculate the Floquet operator  $\mathcal{F}_k$ , which can be directly expressed as

$$\mathcal{F}_k = e^{-i\frac{T}{2}H_k^+} e^{-i\frac{T}{2}H_k^-} \quad (22)$$

Notice that in such a simplified model, there are two controlling parameters  $r$  and  $\xi$ , while the period  $T$  is fixed to be  $\pi$ .  $\xi$  denotes the amplitude of the periodic driving, which originates from self-sustained oscillation in the original nonlinear model.

In spite of the simplicity of this approximation, it could indeed capture the essence of the physics in the original model, especially its phase diagram and the critical behavior. The phase diagram under this step-function approximation is plotted in Fig.1 (b), where the phase boundary is determined by the condition  $\cos[\pi r_c \sqrt{1 - \xi^2}] = -\xi$ , at which the  $\pi$ -mode start to be unstable. Notice that  $r_c \rightarrow \frac{1}{2}$  when  $\xi \rightarrow 0$ , which agrees with our numerical simulation of the nonlinear GLVE.

### CRITICAL DYNAMICS AT THE EXCEPTIONAL POINT

In this section, we provide more details about the explanation of the  $t^{\frac{1}{2}}$  divergence of the average deviation  $\bar{\sigma}(t)$  observed at the critical point, which can be understood as a collective behavior of the k-modes close to  $k = \pi$ .

$$\bar{\sigma}^2(t) = \frac{1}{L} \sum_i \delta_i(t) \delta_i(t) = \frac{1}{L} \sum_k \delta_k(t) \delta_{-k}(t) \quad (23)$$

where the momentum summation is over the k-mode in the first Brillouin Zone  $k \in [0, 2\pi]$  and  $\delta_k(t) = [\delta_k^x(t), \delta_k^y(t)]^T$ .

Right at the critical point, we first focus on the  $\pi$ -mode, whose stroboscopic dynamics is governed by the

Floquet operator

$$\mathcal{F}_\pi = 2\xi \begin{bmatrix} 1 & -1 \\ 1 & -1 \end{bmatrix} + \begin{bmatrix} -1 & 0 \\ 0 & -1 \end{bmatrix} \quad (24)$$

Mathematically, exceptional point means that  $\mathcal{F}_\pi$  has only one eigenvector with an eigenvalue  $-1$ . Next, we will study the long-time dynamics governed by  $\mathcal{F}_\pi$ .

The stroboscopic dynamics of  $\delta_\pi(t)$  with  $t = nT$  ( $T$  is the period) can be directly expressed as

$$\delta_\pi(nT) = \mathcal{F}_\pi^n \delta_\pi(0) \quad (25)$$

Assuming that initially  $\delta_\pi(0) = [a, b]^T$ , from Eq.(25), one can derive that

$$\delta_\pi(t) = (-1)^n \left\{ a \begin{bmatrix} 1 - Kt \\ -Kt \end{bmatrix} + b \begin{bmatrix} Kt \\ 1 + Kt \end{bmatrix} \right\} \quad (26)$$

where  $t = nT$ ,  $K = \frac{2\xi}{T}$ . In the long time limit  $t \gg 1/K$ , Eq.(27) is reduced to:

$$\delta_\pi(t) = (b - a)Kt \begin{bmatrix} 1 \\ 1 \end{bmatrix} \quad (27)$$

which indicates a linear divergence of  $|\delta_\pi(t)|$  at the critical point. This agrees very well with the numerical results as shown in Fig.4, where the envelope of  $|\delta_\pi(t)|$  growth linearly in time.

According to Eq.(23), all the  $k$ -modes contribute to  $\bar{\sigma}(t)$ , while at the critical point, only the  $\pi$ -mode and those  $k$ -mode close to it dominate the long-time dynamics of  $\bar{\sigma}(t)$ . Now we focus on those  $k$ -modes close to  $\pi$ -mode with  $k = \pi + q$  and  $q \ll 1$ . As shown in Fig.4, for a  $k$ -mode that slight deviates from  $k = \pi$ , the envelope of  $|\delta_{\pi+q}(t)|$  behavior resembles a sine function: initially, it grows linearly in time, while after a characteristic time scale  $t_q^*$ , it will significantly deviate from the linear function. Such a characteristic time scale is roughly a quarter of the period of the sine function, which in turns, is proportional to  $1/|q|$ , as shown in Fig.4.

As a consequence, the closer a  $k$ -mode is to  $k = \pi$ , the longer it can contribute to the linear growth dynamics. In another word, at a fixed time  $t$ , only those  $k$ -modes satisfying  $t_q^* > t$  can still contribute to the linear growth. Considering the fact that the  $k$ -modes are equally spaced in the momentum space, we can find that the number of those  $k$ -mode contributing to the linear growth decay in time as  $\mathcal{N}(t) \sim 1/t$ . In summary, at long time, the summation in Eq.(23) can be approximately replaced by the summation over those  $k$ -modes that still contribute to the linear growth

$$\bar{\sigma}^2(t) = \frac{1}{L} \sum_k |\delta_k(t)|^2 \sim \sum_q |\delta_{\pi+q}(t)|^2 \quad (28)$$

where the summation of is over those  $\mathcal{N}(t)$   $k$ -modes, each of which is still growing linearly at time  $t$   $|\delta_{\pi+q}(t)| \sim t$ . Therefore, one can obtain  $\bar{\sigma}(t) \sim t^{\frac{1}{2}}$ , which agrees with our numerical results in the nonlinear GLVE.

## PSEUDO-HERMITICITY OF THE EFFECTIVE HAMILTONIAN

A non-Hermitian Hamiltonian with real spectre is known as pseudo-Hermitian. Here, we will prove that the Hamiltonian proposed in the maintext belongs to a subclass of pseudo-Hermitian Hamiltonian. Mathematically, a Hamiltonian  $H$  is pseudo-Hermitian if it satisfies:

$$H^\dagger = \eta^{-1} H \eta \quad (29)$$

where  $\eta$  is a Hermitian matrix. The Hamiltonian in the present study takes the form as:

$$H = VD \quad (30)$$

where both  $V$  and  $D$  are Hermitian. Thus we have

$$H^\dagger = DV = DVDD^{-1} = DHD^{-1} \quad (31)$$

As a consequence,  $H$  satisfies the pseudo-Hermitian condition (29) with  $\eta = D^{-1}$ .

## AN APPLICATION IN QUANTUM SYSTEM: THE BDG EQUATION FOR QUADRATIC BOSONIC SYSTEM

In this section, we discuss a possible application of our results to a genuine quantum system. Even though the Hamiltonian of this model is Hermitian, its equation of motion takes the same form of a Schrodinger Equation, but with a non-Hermitian Hamiltonian, which is due to the commutation relation between the bosonic operators.

Considering a quadratic bosonic system with the Hamiltonian:

$$H = \omega a^\dagger a + \Delta(a^\dagger a^\dagger + aa) \quad (32)$$

The BdG equation of motion can be expressed as:

$$i \frac{d}{dt} \begin{pmatrix} a \\ a^\dagger \end{pmatrix} = \begin{pmatrix} \omega & \Delta \\ -\Delta & -\omega \end{pmatrix} \begin{pmatrix} a \\ a^\dagger \end{pmatrix}, \quad (33)$$

Formally, Eq.(33) resemble the Schrodinger Equation  $i \frac{\partial \psi}{\partial t} = \tilde{H} \psi$ , where  $\tilde{H}$  is a non-Hermitian matrix that can be expressed as:  $\tilde{H} = DH_0$  with

$$H_0 = \begin{bmatrix} \omega & \Delta \\ \Delta & \omega \end{bmatrix}, D = \begin{bmatrix} 1 & \\ & -1 \end{bmatrix} \quad (34)$$

where both  $H_0$  and  $D$  are Hermitian. If  $\omega > |\Delta|$ ,  $H_0$  is positive definite, thus  $\tilde{H}$  satisfies the condition proposed in the maintext, thus its spectre are real, which indicates that the dynamics of the BdG Eq.(33) are stable. On the contrary, for  $\omega < |\Delta|$ , one of the eigenvalue of  $H_0$  become negative, thus the neither  $H_0$  nor  $D$  are positive definite, and  $\tilde{H}$  has a pair of complex eigenvalues with the opposite imaginary part. Physically, this corresponds to the parametric instability of the quadratic bosonic systems.

More generally, it is easy to generalize the quadratic Hamiltonian (32) into a lattice system, where similar argument can be used to analyze the stability of these systems. The similarity between the BdG equations and the Schrodinger Equation with non-Hermitian Hamilto-

nian provides a new perspective to analyze these kinds of bosonic systems, where intriguing phenomena originated in non-Hermitian physics (*e.g.* the skin effect) might be explored in such a Hermitian quantum system.